IET Intelligent Transport Systems

Research Article

Improving performance of pedestrian positioning by using vehicular communication signals

ISSN 1751-956X
Received on 21st April 2017
Revised 15th November 2017
Accepted on 15th January 2018
doi: 10.1049/iet-its.2017.0134
www.ietdl.org

Suhua Tang[1] ✉, *Sadao Obana*[1]
[1]*Graduate School of Informatics and Engineering, The University of Electro-Communications, Tokyo, Japan*
✉ *E-mail: shtang@uec.ac.jp*

Abstract: Pedestrian-to-vehicle communications, where pedestrian devices transmit their position information to nearby vehicles to indicate their presence, help to reduce pedestrian accidents. Satellite-based systems are widely used for pedestrian positioning, but have much degraded performance in urban canyon, where satellite signals are often obstructed by roadside buildings. The authors propose a pedestrian positioning method, which leverages vehicular communication signals and uses vehicles as anchors. The performance of pedestrian positioning is improved from three aspects: (i) channel state information instead of received signal strength indicator (RSSI) is used to estimate pedestrian-vehicle distance with higher precision. (ii) Only signals with line-of-sight path are used, and the property of distance error is considered. (iii) Fast mobility of vehicles is used to get diverse measurements, and Kalman filter is applied to smooth positioning results. Extensive evaluations, via trace-based simulation, confirm that (i) fixing rate of positions can be much improved. (ii) Horizontal positioning error can be greatly reduced, nearly by one order compared with off-the-shelf receivers, by almost half compared with RSSI-based method, and can be reduced further to about 80 cm when vehicle transmission period is 100 ms and Kalman filter is applied. Generally, positioning performance increases with the number of available vehicles and their transmission frequency.

1 Introduction

On the roads dominated by high-speed vehicles, pedestrians are susceptible to injury or even death in the collisions with vehicles, and are known to be 'weak in traffic'. Annual report of traffic accident statistics [1] shows that 35% traffic fatalities in Japan are pedestrians.

Many efforts have been devoted to reducing pedestrian accidents, as follows: (i) A vehicle itself detects pedestrians by using millimetre-wave-radar or stereo cameras. (ii) A road helps to detect pedestrians by roadside sensors and notifies vehicles by road-to-vehicle communications. (iii) A pedestrian estimates his own position and sends to nearby vehicles by pedestrian-to-vehicle communications (PVCs) [2]. In these three typical methods, vehicles, roads and pedestrians play the main role, respectively. Among these techniques, PVC does not require roadside infrastructure and works well even in the lack of line of sight (LOS), and is the focus of our work. However, its effect heavily depends on the performance of pedestrian positioning.

Global navigation satellite system (GNSS)-based positioning [3] is widely used in mobile devices of pedestrians, and accurately measuring the range between a receiver and a satellite usually requires an LOS path. In urban canyon, however, the LOS path might be obstructed by roadside buildings, and then a GNSS receiver receives a reflected signal instead. This results in a large error in measured range, which cannot be well removed by augmentation techniques such as differential global positioning system and remains the largest error source in urban areas. Many efforts have been devoted to remove reflected signals before fixing absolute positions, including antenna design, correlator refinement (narrow correlator [4], early-late slope correlator, strobe correlator), modulation design (binary offset carrier in modern GPS [5]), carrier smoothing (Hatch filter [6]), signal separation (multipath estimating delay lock loop [7], spatial sampling via antenna array [8]), detection of LOS path (using a 3D geographic information system (GIS) database [9] or an omnidirectional infrared camera [10]). Removing all reflected signals, however, might lead to a shortage of satellites in fixing positions because few satellites are directly visible in urban canyons.

The above problem is common to vehicles and pedestrians, but vehicles have more practical solutions. Vehicles moving on the roads usually see more satellites than pedestrians moving on the sidewalk near roadside buildings. In addition, vehicles have other auxiliary means to improve their position precision with different sensors. In the moving (longitudinal) direction, vehicle's speed can be accurately measured by a speedometer and used for dead reckoning. In the vertical (lateral) direction, vehicle positions can be constrained to roads by map matching, and further constrained to lanes by using cameras or light detection and ranging (LiDAR) for lane detection. In [11], a method is suggested to integrate 3D map (for detecting LOS path of satellite signals), inertial measurement unit (IMU) (for measuring moving direction), speedometer and camera-based lane detection via a particle filter. This method achieves an average positioning error of 0.75 m in the urban area of Tokyo, although its instantaneous error may be as large as 3 m. This indicates the feasibility of precise positioning for vehicles even in urban areas, and the development of autonomous driving surely will further improve the positioning precision of vehicles.

In this paper, we propose to leverage vehicles as anchors to improve the performance of pedestrian positioning in urban canyons. Vehicular communications, which were studied and standardised in the past decade [12, 13], have been put into practical use in Japan since 2015 and will be put into use in USA soon. In this application, vehicles periodically broadcast their position information to avoid collision accidents. In our work, it is assumed that a pedestrian device can overhear signals from vehicles, estimate its distances to vehicles and compute its own position on this basis. Using vehicles as anchors helps to solve the problem of satellite shortage. Fig. 1 shows an image of the proposed method. Signals from vehicles (A and C) with LOS path are used to compute the position of a pedestrian with high precision. Then, this position information is sent to all vehicles including those (B) without LOS paths, by the reflection and/or diffraction of wireless signals. It should be noted that besides vehicles, road side units sharing the same communication protocols can also be used as anchors.

Signals from vehicles to pedestrians are susceptible to attenuation and random fading, and overall signal strength (RSSI: received signal strength indicator) fluctuates even when the distance is the same. In our work, the performance of pedestrian

This is an open access article published by the IET under the Creative Commons Attribution License
(http://creativecommons.org/licenses/by/3.0/)

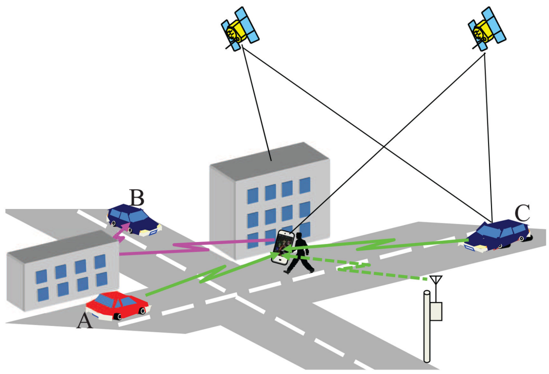

Fig. 1 *Using vehicles (and roadside units) as anchors to improve the performance of pedestrian positioning. Signals from vehicles (A and C) with LOS path are used to compute the position of a pedestrian with high precision. Then, this position information is sent to all vehicles including those (B) without LOS paths, by the reflection and/or diffraction of wireless signals.*

positioning is improved from three aspects, as follows: (i) channel state information (CSI) instead of RSSI is used to estimate pedestrian-vehicle distance with higher precision. (ii) Only signals with LOS paths are used, and the property of distance errors is considered. (iii) Fast mobility of vehicles is used to get diverse measurements, and Kalman filter is applied to smooth positioning results. Part of (i) and (ii) has been reported in [14], and is enhanced in this paper as follows: (i) support vector regression (SVR) is used to estimate distance from CSI, and (ii) the property that errors in estimated distance increase with distances is leveraged to weight distances in computing positions. Extensive evaluations, via trace-based simulation, confirm that the proposed method improves both fixing rate and positioning precision. Horizontal positioning error is greatly reduced, nearly by one order compared with off-the-shelf receivers, by almost half compared with RSSI-based method, and is reduced further to about 80 cm when vehicle transmission period is 100 ms and Kalman filter is applied.

This paper is organised as follows. Section 2 introduces related work and Section 3 explains the motivation. Section 4 presents the proposed method for pedestrian positioning. Then, Section 5 gives the evaluation result, including both distance estimation and positioning precision. Finally, Section 6 concludes this paper.

2 Related work

Precision of pedestrian positioning usually is improved from three aspects, as follows:

i. In outdoor environments, pedestrian positioning mainly depends on satellite signals, and a straightforward method is to improve the number of available satellites, which is possible by leveraging not only GPS but also GLONASS, Galileo, Beidou, and QZSS [15]. However, in urban canyons, the available satellites usually are located overhead, which limits the improvements.
ii. Mobile devices of pedestrians usually are equipped with multiple sensors, based on which pedestrian dead-reckoning becomes available [16]. To remove the accumulated error, however, the position must be corrected by using satellite signals.
iii. Indoor positioning has attracted much research interest recently, and leverages short-range wireless communications such as Wi-Fi [17, 18]. Typically, these methods use either fingerprint [19] or trilateration. As for the latter, the positions of Wi-Fi access points (APs) are assumed to be known. In conventional trilateration methods, the distance between a user and an AP is estimated based on the attenuation property of RSSI with respect to distance. However, RSSI is usually susceptible to multipath fading which leads to a large distance error. Recently, it is suggested to extract the LOS component from CSI information [20] instead of using RSSI. However, its performance is limited by the time resolution of off-the-shelf Wi-Fi modules because of limited channel bandwidth. A solution to this problem is to let a mobile device and its associated AP hop over all Wi-Fi channels to collect channel state over a very wide band [21], and on this basis, get a fine time resolution [22] to achieve decimetre-level localisation, at the cost of sacrificing the communication performance and causing a large delay in positioning. With multiple antennas being available at an AP, each AP can estimate the direction of a pedestrian. With multiple APs connected via a centralised server, the position of a pedestrian can be computed at the server by using all the direction information [23]. However, this is not applicable to compute pedestrian position in a distributed way.

3 Motivations

Precision of GNSS-based positioning depends on the performance of ranging and the distribution of satellites in the sky. In this work, we use mobile vehicles as anchors (pseudo-satellites) to improve the precision of pedestrian positioning. In the following, we take a comparison between satellites and vehicles in terms of their roles as anchors.

i. *Placement and availability*. High precision positioning requires a good placement of anchors, which decides dilution of precision (DOP). From the viewpoint of DOP, satellites with low elevation angles are desired, but are more susceptible to obstruction in urban canyon. On the other hand, satellites with high elevation angles are less susceptible to obstruction, but limiting the distribution of satellites overhead will lead to a high DOP, and potentially large errors. In comparison, vehicles are on the road with nearly zero elevation angles. Although LOS paths between some vehicles and a pedestrian also may be obstructed temporarily, there are many other vehicles available with LOS paths.
ii. *Precision of ranging*: The range between a satellite and a pedestrian is relatively accurate in the presence of LOS path. In comparison, ranging accurately between vehicles and a pedestrian is a challenge and standalone positioning is not so accurate.
iii. *Dynamics*: Owing to a very long distance between a satellite and a pedestrian, the relative direction of a satellite does not change very much within a short time. In other words, the obstruction of a satellite by roadside buildings cannot be removed quickly. In contrast, vehicles move fast, and their topology changes greatly within a short time. Meanwhile vehicles transmit signals periodically (default period is 100 ms). The frequent measurements at different locations compensate for the inaccuracy of pedestrian-vehicle distances. The combination with dead-reckoning by Kalman filtering helps to further improve the precision of pedestrian position.

4 Framework for pedestrian positioning

Fig. 2 shows our system framework for pedestrian positioning. A pedestrian mobile device is equipped with a GNSS receiver and a single radio (single antenna). Via this radio, a pedestrian device

This is an open access article published by the IET under the Creative Commons Attribution License (http://creativecommons.org/licenses/by/3.0/)

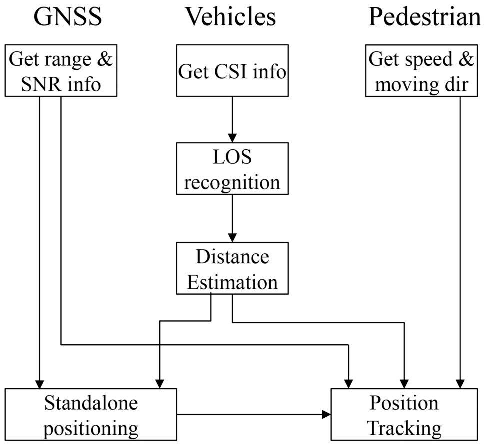

Fig. 2 *System model of pedestrian positioning. It uses three kinds of information, and two positioning mode. In standalone mode, the position is computed by using signals from GPS satellites and/or vehicles. In the tracking mode, Kalman filter is further used to smooth the positioning results by using pedestrian speed*

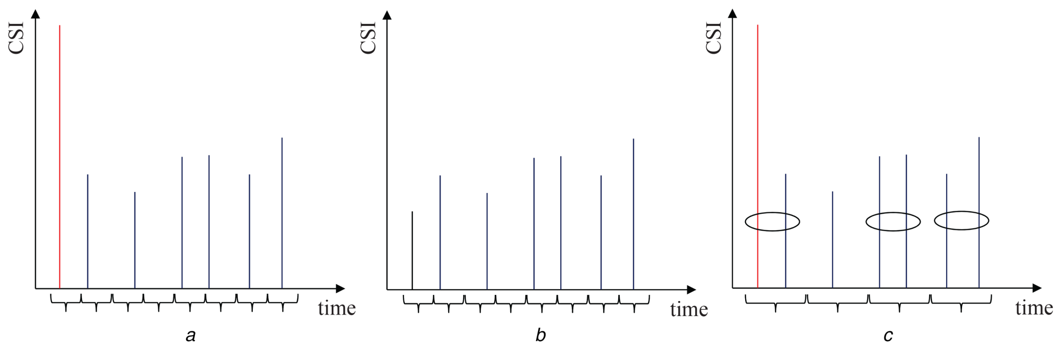

Fig. 3 *CSI in the time domain*
(a) LOS component exist (the leftmost line), ***(b)*** LOS component does not exist, ***(c)*** Different components overlap in a coarse time resolution (time difference of arrival of two paths is less than the time resolution)

passively overhears position messages from passing vehicles. Vehicles periodically exchange their position messages, by dedicated short range communications (DSRC) in the 5.9 GHz band or the 700 MHz band, to learn the presence of nearby vehicles and their operations (e.g. sudden break) so as to avoid traffic accidents, or implement more advanced functions such as cooperative adaptive cruise control in the era of autonomous driving. Then, a pedestrian device leverages the following three kinds of information sources to compute its position: GNSS positioning signals, vehicular communication signals, and pedestrian speed and moving direction. The position of a pedestrian can be transmitted to vehicles to let vehicles learn the presence of the pedestrian and avoid potential collisions.

GNSS signal processing uses conventional method, based on which satellite positions, pseudo-ranges and signal-to-noise ratio (SNR) are obtained from off-the-shelf GNSS module. When a signal is received from a vehicle, position and ID of the vehicle are obtained after decoding the signal. In addition, whether the signal contains LOS path or not is detected, and if affirmative, the distance is further estimated.

Since vehicles cannot transmit simultaneously, a pedestrian device will receive messages from different vehicles at different timing while moving. A pedestrian at a walking speed (80 m per min) moves about 13 cm within 100 ms. This distance, compared with the positioning error, is very small. Therefore, a pedestrian is assumed to have the same position within 100 ms, and uses all messages received within 100 ms to compute his position.

Pedestrian position is computed in two modes. In the standalone mode, the position is computed by using GNSS and/or vehicular signals. In the tracking mode, pedestrian speed is further used to smooth the results of consecutive positioning.

4.1 LOS detection and distance estimation

The signal from a vehicle arrives at a pedestrian device as different components via different paths, each with its own propagation delay and signal strength, which is usually represented by CSI [17]. In the presence of a LOS path, the LOS component is the first one that arrives at the pedestrian device, with a relatively stronger strength than subsequent reflected components which have extra attenuation per reflection, diffraction etc. Fig. 3*a* shows an example of CSI where the red line represents the LOS path. On the other hand, in the absence of an LOS path (Fig. 3*b*), the first component is also a reflected or diffracted one, and its signal strength is comparable to the subsequent ones. Such property of CSI is used to detect whether an LOS path exists or not. Then, CSI with LOS component is used to estimate the pedestrian-vehicle distance.

However, this works well only when there is a fine time resolution that can separate all components in their arrival timings. Off-the-shelf radios (DSRC modules) usually have a finite bandwidth (e.g. 10 MHz) and the time resolution is limited (e.g. 100 ns). Equivalently, the time axis is divided into bins (e.g. with a width of 100 ns). Signal components whose arrival timing difference is less than the bin width will overlap in the same bin and are not distinguishable (Fig. 3*c*). In [20], it is suggested that the bin with the largest energy be regarded as the LOS component if the ratio of its energy to that of all bins is above a threshold, and this is evaluated for the indoor environments. However, we found that in road environments this does not work well due to the ground reflection, which can be explained as follows. Assume the heights of a vehicle (transmit) antenna and a pedestrian (receive) antenna are h_t and h_r, respectively, and the pedestrian-vehicle distance is d. Then, the path length difference between the LOS path and ground reflection path [24] is approximately $\Delta = 2 \cdot h_t \cdot h_r / d$, and $\Delta \geq 0.09$ meter when $h_t = 1.5$ m, $h_r = 1.5$ m, and $d \leq 50$ m. This corresponds to a time difference of 0.3 ns, which is far less than the bin width (e.g. 100 ns).

This is an open access article published by the IET under the Creative Commons Attribution License
(http://creativecommons.org/licenses/by/3.0/)

We decide to overcome the limitation of time resolution in two steps. (i) Use machine learning to predict whether LOS exists or not given CSI as input. Both CSI with LOS (Fig. 3*a*) and without LOS (Fig. 3*b*) are collected and annotated, and a recognition model is trained by supervised learning. (ii) Use machine learning to estimate the distance from CSI by regression. Here, each CSI with an LOS component is annotated with its corresponding distance.

CSI is represented by a vector (with a fixed length corresponding to the maximal delay) of complex numbers. Each bin of the CSI vector may be the complex gain of one path or the overall gain (sum) of multiple paths. By initial experiments, we found that both LOS recognition and distance regression are insensitive to the phase information included in the CSI. Therefore, only the amplitude of CSI is computed. In the LOS recognition, the CSI amplitude is further normalised. Distance estimation depends on the attenuation property of wireless signals, and usually the LOS component should be used. When the LOS component is overlapped by subsequent non-LOS component in the same bin, the overall strength fluctuates and affects the distance estimation. Although the LOS component and subsequent non-LOS components propagate via different paths, generally, the longer the distance is, the smaller all CSI bins tend to be. Therefore, we try to train a model to estimate the distance from all bins of a CSI vector, instead of merely using the bin (including the LOS component) with the largest strength. To better fit the propagation model, the CSI amplitude is converted to the log scale (dBm), and the pair of (log distance, log CSI amplitude) is used to train a regression model for predicting the distance from the CSI vector.

4.2 Positioning in the standalone mode

The pseudo-range ($p^{(s)}$) to a satellite (s) is represented as the sum of the true distance ($\rho^{(s)} = |\boldsymbol{r}^{(s)} - \boldsymbol{r}|$, where $\boldsymbol{r}^{(s)}$ and $\boldsymbol{r}$ are the 3D coordinates of satellite s and the pedestrian, respectively), the distance error (δ) due to clock drift of pedestrian device and other errors ($\xi^{(s)}$) caused by extra propagation delay (such as ionosphere, troposphere) [3]

$$p^{(s)} = \rho^{(s)} + \delta + \xi^{(s)}. \tag{1}$$

The estimated distance ($p^{(v)}$) to a vehicle (v) with an LOS path is the sum of the true distance ($\rho^{(v)} = |\boldsymbol{r}^{(v)} - \boldsymbol{r}|$) and the measurement error ($\xi^{(v)}$), as follows:

$$p^{(v)} = \rho^{(v)} + \xi^{(v)}. \tag{2}$$

Equation (1) is generated per satellite and (2) is generated per vehicle. These equations can be rewritten in a vector form ($\boldsymbol{p} = [p^{(1)}; p^{(2)}; \cdots]$, $\boldsymbol{\rho} = [\rho^{(1)}; \rho^{(2)}; \cdots]$, column vectors are stacked by the operator ';')

$$\boldsymbol{p} = \boldsymbol{\rho}(\boldsymbol{r}) + \delta + \boldsymbol{\xi} \tag{3}$$

and approximately linearised at an initial position ($\boldsymbol{r}_0$) as

$$\boldsymbol{p} = \boldsymbol{\rho}(\boldsymbol{r}_0) + \boldsymbol{H}(\boldsymbol{r}_0) \cdot (\boldsymbol{r} - \boldsymbol{r}_0; \delta - \delta_0) + \delta_0 + \boldsymbol{\xi}. \tag{4}$$

Neglecting the measurement error in pseudo-ranges and distances, pedestrian position $\boldsymbol{r}$ (and clock error δ) can be iteratively computed as

$$[\boldsymbol{r}_{i+1} - \boldsymbol{r}_i; \delta_{i+1} - \delta_i] = (\boldsymbol{H}_i^{\mathrm{T}}\boldsymbol{H}_i)^{-1}\boldsymbol{H}_i^{\mathrm{T}} \cdot (\boldsymbol{p} - \boldsymbol{\rho}(\boldsymbol{r}_i) - \delta_i). \tag{5}$$

Pseudo-ranges to satellites and distances to vehicles have different error properties, and should be treated differently in positioning by using different weights. Let the covariance matrix of $\boldsymbol{\xi}$ be $\boldsymbol{R}$. Then, $\boldsymbol{R}^{-1}$ can be assigned to pseudo-ranges/distances as weights, with a small weight for pseudo-ranges/distances with large errors

$$[\boldsymbol{r}_{i+1} - \boldsymbol{r}_i; \delta_{i+1} - \delta_i] = (\boldsymbol{H}_i^{\mathrm{T}}\boldsymbol{R}^{-1}\boldsymbol{H}_i)^{-1} \cdot \boldsymbol{H}_i^{\mathrm{T}}\boldsymbol{R}^{-1} \cdot (\boldsymbol{p} - \boldsymbol{\rho}(\boldsymbol{r}_i) - \delta_i). \tag{6}$$

Typically, $\boldsymbol{R}$ is a diagonal matrix and the diagonal elements of $\boldsymbol{R}^{-1}$ are weights (w). However, these diagonal elements are unknown and change over time. As for satellites, signals with an LOS path typically have high SNR and small ranging errors, but reflected signals with low SNR have large ranging errors. Therefore, a heuristic method is to associate SNR (γ) with weights. First, an SNR threshold (γ_{th}) is set to remove all signals whose SNR is below this threshold (potentially without an LOS path). Then, for all usable satellites, a weight is set to be proportional to the SNR difference ($\gamma - \gamma_{\mathrm{th}}$), a larger value for satellites with larger SNR. As for vehicles, errors in distance estimation increase with distances, which is analysed in [14] and confirmed in Section 5.2. Therefore, a large weight is used for a short estimated distance.

Only the computation leading to a convergence (i.e. $|\boldsymbol{r}_{i+1} - \boldsymbol{r}_i|$ approaches 0) is regarded as a successful position fixing. As will be discussed later, combining signals from GPS and vehicles may even lead to larger errors sometimes. Therefore, from the positions computed by GPS, vehicles, GPS and vehicles, the one with the least average residual is selected

$$\text{residual} = \frac{1}{|\boldsymbol{p}|}\sum_{i=1}^{|\boldsymbol{p}|} w_i \cdot |p^{(i)} - \rho^{(i)}(\boldsymbol{r}_\infty) - \delta_\infty|. \tag{7}$$

4.3 Position tracking

Position tracking is realised by a Kalman filter, using the speed information of a pedestrian to smooth positioning results. The state of the Kalman filter, $\boldsymbol{X}_t = [\boldsymbol{r}_t; \boldsymbol{v}_t; \dot{\boldsymbol{v}}_t; \delta_t]$, consists of pedestrian position $\boldsymbol{r}_t$, speed $\boldsymbol{v}_t$, acceleration $\dot{\boldsymbol{v}}_t$, and clock error δ_t at time t. According to the relationship between position, speed, and acceleration ($\boldsymbol{r}_t = \boldsymbol{r}_{t-\Delta t} + \boldsymbol{v}_t \cdot \Delta t$, $\boldsymbol{v}_t = \boldsymbol{v}_{t-\Delta t} + \dot{\boldsymbol{v}}_t \cdot \Delta t$), the evolution of state $\boldsymbol{X}_t$ can be represented by a matrix $\boldsymbol{\Phi}$, with a random vector $\boldsymbol{w}_{t-\Delta t}$ indicating potential variations, as follows:

$$\begin{aligned} \boldsymbol{X}_t &= \boldsymbol{\Phi}\boldsymbol{X}_{t-\Delta t} + \boldsymbol{w}_{t-\Delta t}, \\ \boldsymbol{\Phi} &= \begin{bmatrix} \boldsymbol{I} & \Delta t \cdot \boldsymbol{I} & & \\ & \boldsymbol{I} & \Delta t \cdot \boldsymbol{I} & \\ & & \boldsymbol{I} & \\ & & & 1 \end{bmatrix}. \end{aligned} \tag{8}$$

The variance of $\boldsymbol{w}_{t-\Delta t}$, denoted as $\boldsymbol{Q}$, is nearly stationary.

The measurement $\boldsymbol{Y}_t = [\boldsymbol{p}_t; \boldsymbol{v}_t]$ contains pseudo-range and distance ($\boldsymbol{p}_t$) and pedestrian speed ($\boldsymbol{v}_t$), and is indirectly associated with the state $\boldsymbol{X}_t$ by the following equation:

$$\boldsymbol{Y}_t = [\boldsymbol{\rho}_t + \delta_t; \boldsymbol{v}_t] + \boldsymbol{\xi}_t. \tag{9}$$

$\boldsymbol{Y}_t$ can be linearised near a state $\boldsymbol{X}_t$, where a small change $\partial\boldsymbol{X}_t$ leads to a change $\boldsymbol{H}_t \cdot \partial\boldsymbol{X}_t$ in $\boldsymbol{Y}_t$. $\boldsymbol{R}$, the variance of $\boldsymbol{\xi}_t$, changes with time and is set empirically, as discussed in the previous section.

The process of updating state $\boldsymbol{X}_t$ and its variance $\boldsymbol{P}_t$ for a pedestrian is briefly described as follows [25]:

- *Pedestrian state prediction*: New state $\boldsymbol{X}_t^-$ (and position $\boldsymbol{r}_t^-$) of a pedestrian is predicted from the past position and moving speed

$$\boldsymbol{X}_t^- = \boldsymbol{\Phi}\boldsymbol{X}_{t-\Delta t}^+, \quad \boldsymbol{P}_t^- = \boldsymbol{\Phi}\boldsymbol{P}_{t-\Delta t}^+\boldsymbol{\Phi}^{\mathrm{T}} + \boldsymbol{Q}. \tag{10}$$

- *Pseudo-range and distance estimation*: From the predicted pedestrian position, pseudo-ranges to satellites and distances to vehicles are estimated. $p_t^{(s)-}$ is computed from $\rho_t^{(s)} = |\boldsymbol{r}_t^- - \boldsymbol{r}_t^{(s)}|$ by adding clock error for satellites.
- *Pedestrian state update*: Kalman gain $\boldsymbol{K}_t$ is computed based on the variance ($\boldsymbol{P}_t^-$) of predicted information and the variance $\boldsymbol{R}$ of measured information. Then, the predicted state $\boldsymbol{X}_t^-$ is updated to its new value $\boldsymbol{X}_t^+$ by adding the prediction error $\boldsymbol{Y}_t - (\boldsymbol{p}_t^-; \boldsymbol{v}_t^-)$ weighted by the Kalman gain, and pedestrian position $\boldsymbol{r}_t^+$ is obtained from $\boldsymbol{X}_t^+$

This is an open access article published by the IET under the Creative Commons Attribution License
(http://creativecommons.org/licenses/by/3.0/)

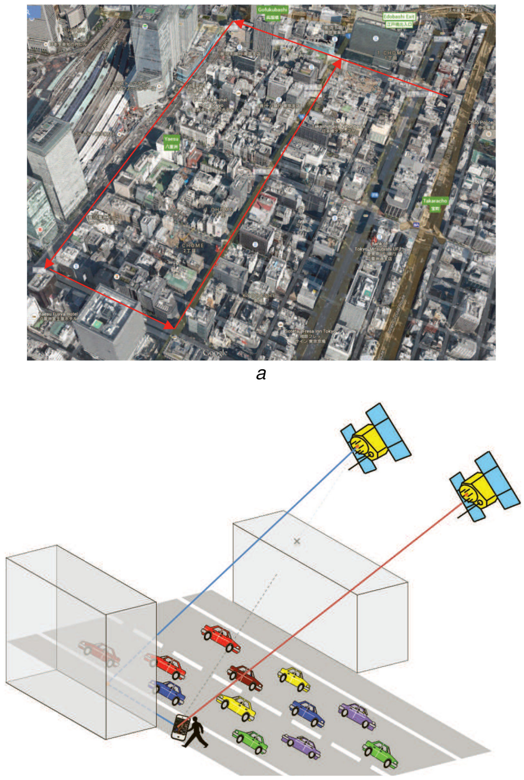

a

b

Fig. 4 *Evaluation scenario*
(a) Moving route for collecting GPS trace data, ***(b)*** Scenario for simulation evaluation

$$\boldsymbol{K}_t = \boldsymbol{P}_t^- \cdot \boldsymbol{H}_t^{\mathrm{T}} \cdot [\boldsymbol{H}_t \cdot \boldsymbol{P}_t^- \cdot \boldsymbol{H}_t^{\mathrm{T}} + \boldsymbol{R}], \tag{11}$$

$$\boldsymbol{X}_t^+ = \boldsymbol{X}_t^- + \boldsymbol{K}_t \cdot [\boldsymbol{Y}_t - (\boldsymbol{p}_t^-; \boldsymbol{v}_t^-)], \quad \boldsymbol{P}_t^+ = (\boldsymbol{I} - \boldsymbol{K}_t\boldsymbol{H}_t)\boldsymbol{P}_t^-. \tag{12}$$

5 Evaluation by trace-based simulation

Here, we first introduce the trace data used for simulation evaluation. Then, we present the results of LOS recognition and distance estimation, and show the impact of different factors (e.g. vehicle density) on the positioning performance.

5.1 Evaluation setting

GPS trace data (ephemeris for computing satellite positions, measured pseudo-ranges after removing ionosphere, troposphere impact) is collected by a high sensitivity receiver [u-blox EVK-6T]. This receiver is mounted on an experiment car near to a high precision multi-GNSS receiver, which is equipped with high performance gyro to obtain a ground truth position with an error less than 10 cm. The experiment car is moved along the lane near the sidewalk around Tokyo station, following the route shown in Fig. 4*a*. This mimics a walking pedestrian with a GPS receiver. There are high buildings on both sides of the road, which greatly degrade the positioning precision of a plain pedestrian device.

As for pedestrian trace collection, we use two desktop PCs, one for mimicking vehicle and the other for mimicking pedestrian. Due to the lack of DSRC modules, we adopt the Intel 5300 commodity Wi-Fi card with external antennas and use the CSI collection tool [26]. Since desktop PCs require stable power supply, we choose to collect this trace on the road of our campus. The CSI tool exploits the OFDM modulation to collect the channel frequency response (complex gain of 30 equally spaced sub-carriers) of a 20 MHz channel in the 2.4 GHz band. On this basis, CSI is obtained by the inverse Fourier transform. This collected pedestrian trace is divided into two parts: one with LOS path and the other without LOS path, each of which is indexed by the actual distance.

We use the scenario in Fig. 4*b* and main parameters in Table 1 to set up the trace-based simulation, by the following steps: (i) Satellite positions, pseudo-ranges and SNR are extracted from the GPS trace, and currently only GPS satellites are used. Elevation angle mask is set to 20° and SNR threshold is set to 40 dB. (ii) We use a road with two lanes per direction, and each vehicle moves along a lane at a fixed speed. Inter-vehicle distance is adjusted to change vehicle density. A pedestrian moves along the left sidewalk. Actual vehicle-pedestrian distance is computed. Vehicles with distances less than an LOS distance threshold (12 m) are regarded as directly visible with LOS path. Beyond this distance threshold, whether a vehicle has an LOS path is randomly determined based on a configurable LOS probability. Then, for each vehicle, according to its LOS flag, the corresponding pedestrian trace (with/without LOS) is determined. From the CSI entries that have the distances nearest to the vehicle-pedestrian distance, one CSI is randomly selected. Finally, vehicle position is adjusted a little along its moving direction so that the pedestrian-vehicle distance matches that of CSI. (iii) Random error is generated and added to 2D pedestrian speed. More specifically, uniform errors, in the range [−1, 1] m/s when the pedestrian moves forward and in the range [−2, 2] m/s when the pedestrian turns around, are added to both the moving and vertical directions.

It is known that in the urban areas, errors in GPS-based positioning can be as large as few tens of meters, because most satellites are not directly visible and a receiver (with high sensitivity) will use pseudo-ranges with multipath errors. In our evaluation, there are many more passing vehicles than satellites. Based on the literature [11], we assume that vehicles have accurate position (with very small errors). The CSI information of each vehicle is used for LOS recognition and distance estimation via regression. In this way, non-LOS signals are removed, and the distance accuracy is improved. Only vehicles whose estimated distance are no more than positioning distance threshold (50 m) and all satellites whose SNR is no less than SNR threshold (40 dB) are used to compute pedestrian position. The weight for each vehicle is determined based on its estimated distance. By all these means, we can greatly reduce the positioning error of pedestrians to the meter level.

This is an open access article published by the IET under the Creative Commons Attribution License
(http://creativecommons.org/licenses/by/3.0/)

Table 1 Main parameters for simulation

	Parameter	Value
GPS	elevation angle mask	20°
	SNR threshold	40 dB
vehicle	number of lanes per direction	2
	vehicle speed	50 km/h
	inter-vehicle distance	variable (default = 40 m)
	LOS distance threshold	12 m
	LOS probability	variable (default = 0.6)
	positioning distance threshold	50 m
	vehicle transmission period	variable (default = 1 s)
speed error	go forward (longitudinal/lateral)	uniform in [−1, 1]m/s
	turn around (longitudinal/lateral)	uniform in [−2, 2]m/s

Table 2 Performance of LOS recognition by support vector machine

	With LOS	Without LOS
with LOS	0.912	0.088
without LOS	0.080	0.920

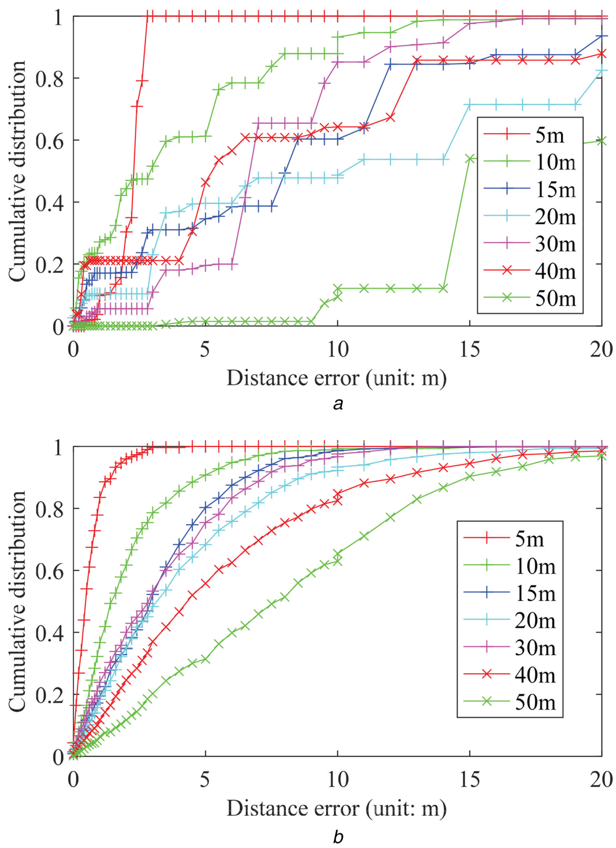

Fig. 5 *Cumulative distribution function of distance errors of signals with LOS path under different distance ranges*
(a) RSSI based (linear regression), ***(b)*** CSI based (SVR)

5.2 Evaluation of LOS recognition and distance estimation

We selected support vector machine with the radial basis function (RBF) kernel to train a classifier to predict from CSI information whether a signal contains an LOS path or not. We randomly split the CSI data (altogether 3784 entries) into two parts: 75% for training and 25% for testing. The results, averaged over 10 cross validations, are shown in Table 2. The accuracy is high and false-positive probability (without LOS → with LOS) is low.

We selected SVR with the RBF kernel to train a model for estimating distance from CSI, using all CSI data (altogether 1838 entries) with LOS paths. For a comparison, we also used linear regression between the log values of distances and RSSI to estimate distance from RSSI. The cumulative distribution functions (CDFs) of distance errors of signals with LOS path, by using RSSI-based method and CSI-based method, are shown in Figs. 5*a* and *b*, respectively. When SVR is used, there is a clear trend that distance error increases with distance, which is consistent with the analysis in [14]. Generally, the mean error of SVR-based method is nearly half of that of RSSI-based method. It should be noted that signals without LOS path usually have much large errors.

5.3 Evaluation of pedestrian positioning performance

Pedestrian positioning performance depends on the methods of distance estimation. In the following, RSSI and CSI represent RSSI-based (linear regression) and CSI-based (SVR regression) methods, respectively. KF indicates that a Kalman filter is further used, and GPS + CSI means the combination of CSI with GPS. In this evaluation, we focus on two metrics, one is fixing rate (defined

This is an open access article published by the IET under the Creative Commons Attribution License
(http://creativecommons.org/licenses/by/3.0/)

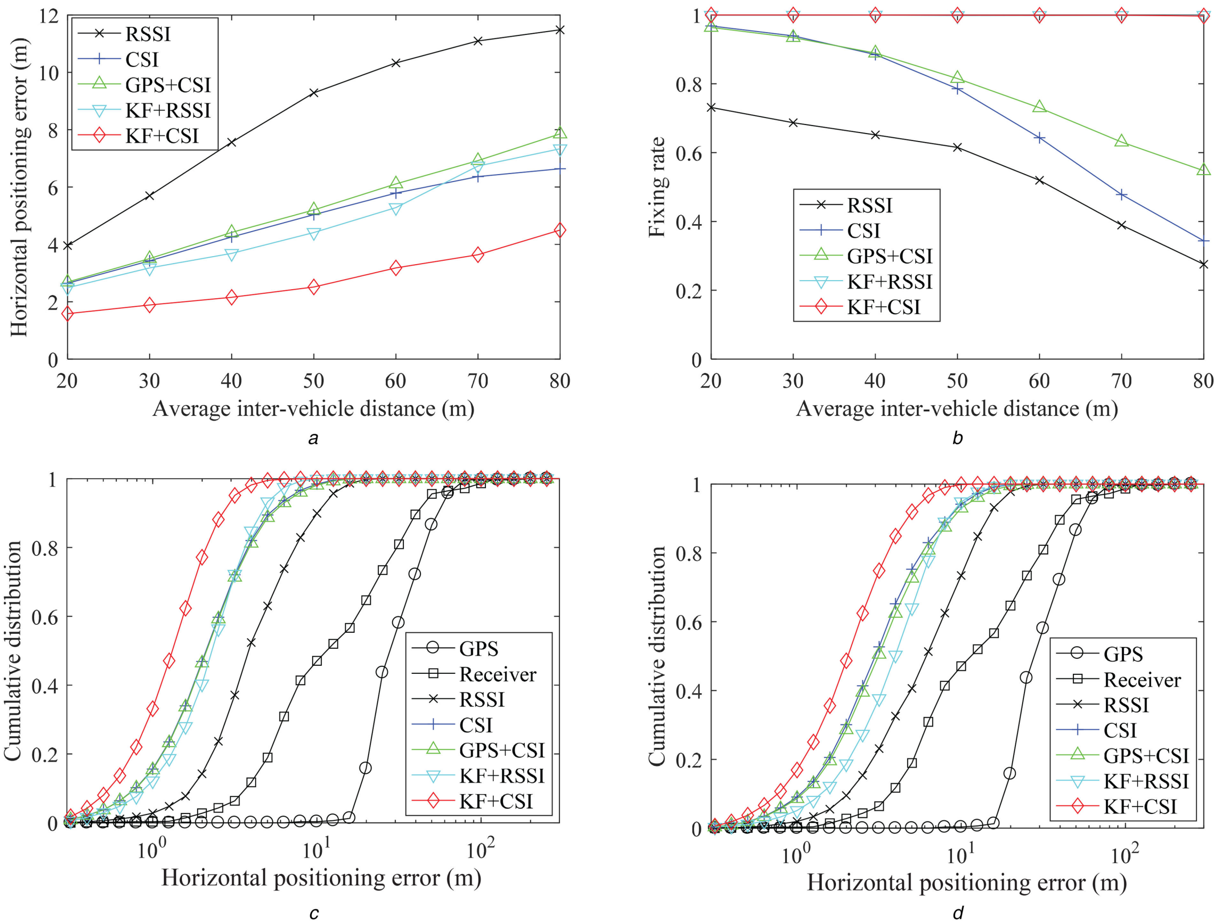

Fig. 6 *Horizontal positioning error and fixing rate under different inter-vehicle distances. Cumulative distribution of horizontal positioning error when inter-vehicle distance is equal to 40 m and 70 m*

(a) Horizontal positioning error (m), ***(b)*** Position fixing rate, ***(c)*** Inter-vehicle distance = 40 m, ***(d)*** Inter-vehicle distance = 70 m

as the percentage of epochs that the positioning computation converges) and the other is horizontal positioning error. First, we assume that the position of each vehicle is correct without error, and later we evaluate the impact of vehicle position errors. Vehicle transmission period is set to 1 s initially, the same as the GPS receiver positioning period. Later we will also evaluate the impact of vehicle transmission period.

5.3.1 Impact of vehicle density (inter-vehicle distance): Pedestrian positioning performance heavily depends on vehicle density (inter-vehicle distance). Figs. 6*a* and *b* show the positioning error and fixing rate, respectively. Generally, a larger inter-vehicle distance (fewer vehicles) leads to larger positioning error. Compared with RSSI-based method, CSI-based method greatly reduces positioning error. Using a Kalman filter helps to reduce positioning error in both KF + RSSI and KF + CSI. When inter-vehicle distance is around 40 m (approximately equal to the required safe distance at the speed of 50 km/h), the positioning error is around 2 m in KF + CSI.

Vehicle density also affects position fixing rate when KF is not used. Usually, a high fixing rate is achieved at a small inter-vehicle distance. An interesting thing is that CSI-based method also improves fixing rate compared with RSSI-based method. This is because by improving the precision of distances in CSI-based method, the convergence rate is improved. Compared with CSI, GPS + CSI improves fixing rate when inter-vehicle distance is relatively large (≥60 m) which confirms that GPS and vehicles complement each other when vehicle density is low.

Positioning errors of these methods are further described by CDFs in Figs. 6*c* and *d*, where inter-vehicle distance is equal to 40 and 70 m, respectively. The results of GPS (recomputed using pseudo-ranges and satellites under the SNR threshold constraint) and receiver (directly obtained from the receiver) are also presented as a reference. Ninety per cent of errors in GPS and receiver are less than 69.2 and 50.1 m, respectively. When inter-vehicle distance is 40 m, 90% errors in RSSI, CSI, GPS + CSI, KF + RSSI, KF + CSI methods are less than 12.6, 6.46, 6.61, 5.62, 3.23 m, respectively. When inter-vehicle distance increases to 70 m, positioning error also increases, and 90% errors in these methods are less than 17.8, 10.2, 10.7, 10.2, 5.75 m, respectively.

5.3.2 Impact of LOS probability: Here we evaluate the impact of LOS probability for vehicles beyond the LOS distance threshold (12 m), and Figs. 7*a* and *b* show the results. Signals from some of the vehicles may be obstructed by other vehicles. For the CSI-based method, by removing non-LOS signals, the number of available vehicles decreases. When vehicle density is high enough, this has little impact. As for the RSSI-based method, non-LOS signals usually lead to an estimated distance greater than the positioning distance threshold (50 m) and are not involved in the position computation. Even some distances with large errors may be falsely used in the position computation, a large estimated distance is assigned a small weight. Therefore, the impact of LOS probability on positioning error is not so large as expected. In comparison, the impact of LOS probability on the fixing rate is a little more obvious. Again GPS + CSI helps to improve positioning rate when few vehicles (with LOS path) can be used.

5.3.3 Impact of vehicle position error: In previous evaluations, it is assumed that vehicle position is correct, without any errors. Actually, it is possible that vehicle positions have a small error. In the case of dead-reckoning, such errors are not random. Here, we set a random initial position error to each vehicle and this error is kept unchanged in each simulation. This corresponds to satellite position error in the GPS system. Fig. 8 shows the result, where the horizontal axis is the maximal error in the moving direction (the maximal error in the vertical direction is set to 20% of that in the moving direction). A large error in vehicle position does lead to a

This is an open access article published by the IET under the Creative Commons Attribution License
(http://creativecommons.org/licenses/by/3.0/)

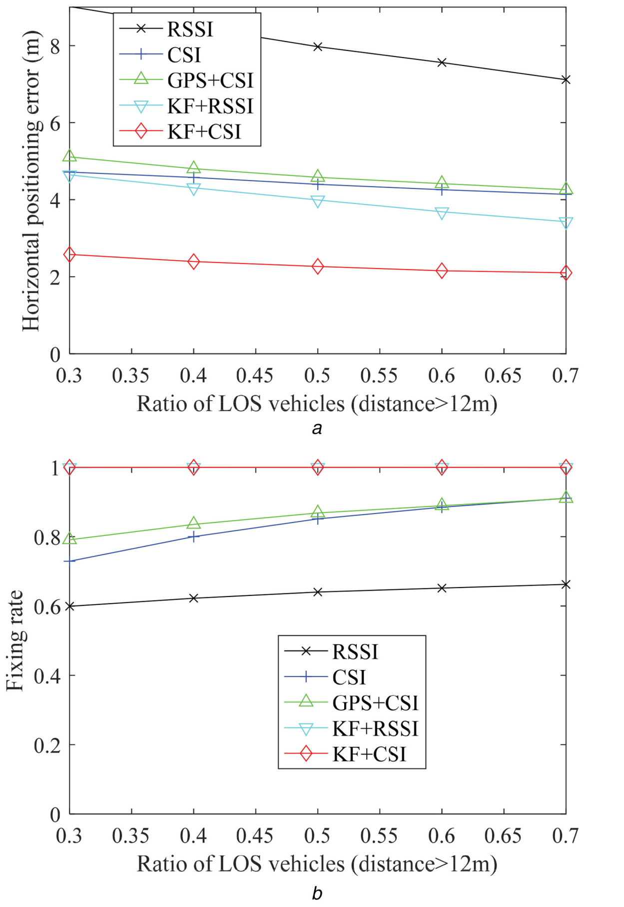

Fig. 7 *Positioning performance under different LOS probabilities (inter-vehicle distance = 40 m)*
(a) Horizontal positioning error (m), ***(b)*** Fixing rate

noticeable error increase in pedestrian position. This is a systematic error, and requires other efforts to improve the positioning precision of vehicles. However, the error increase is almost negligible when maximal vehicle position error is no more than 2 m, and this is achievable in the era of autonomous driving.

5.3.4 Impact of vehicle transmission period: Vehicle transmission period was set to 1 s in previous evaluations, the same as satellite positioning period. Here, we investigate the impact of vehicle transmission period (the maximal error of vehicle position in the moving direction is set to 1 m). Fig. 9 shows the CDF of horizontal positioning error of KF + CSI, where each curve corresponds to a specific vehicle transmission period. It is clear that pedestrian positioning error decreases greatly with vehicle transmission period. This is because with a smaller transmission period, there are more distance measurements. By using a Kalman filter to smooth these measurements, the random error is greatly reduced. This is especially useful when the inter-vehicle distance is relatively large (70 m in Fig. 9*b*). At the transmission period 100 ms, average horizontal positioning error is 0.74 m when inter-vehicle distance is 40 m, and 0.85 m when inter-vehicle distance is 70 m.

In the real environment, the vehicle transmission period depends on whether a vehicle changes its moving direction or speed, and not all vehicles transmit at the period of 100 ms. In the worst case where all vehicles transmit at a period of 1 s, the average positioning error will be relatively large, 1.50 m when inter-vehicle distance is equal to 40 m, and 1.91 m when inter-vehicle distance is equal to 70 m. However, near intersections where accidents happen most frequently, vehicles tend to change their speeds (decelerate to avoid colliding with pedestrians or accelerate to pass the intersection) or directions (turn left or right). If on average each vehicle transmits at a period of 200 ms, a pedestrian device will have enough vehicles as anchors to compute an accurate position. This performance can be further improved by

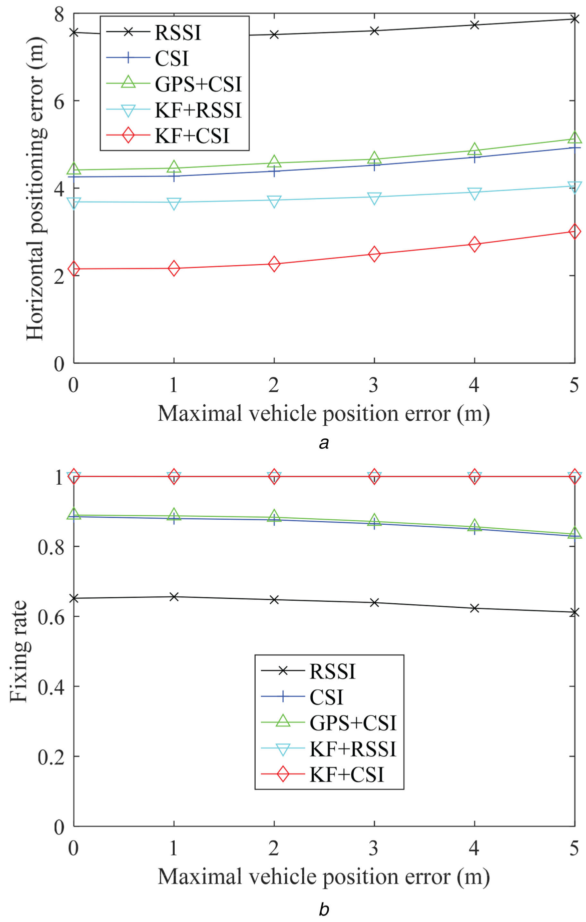

Fig. 8 *Positioning performance under different vehicle position errors (inter-vehicle distance = 40 m)*
(a) Horizontal positioning error (m), ***(b)*** Fixing rate

using road-side units as anchors, and its evaluation is left as a future work.

Based on the above evaluations, we give the following remarks: Vehicles as mobile anchors help to greatly reduce the positioning errors to the meter level. When vehicle position error is no more than 1 m, and each vehicle on average transmits at a period of 200 ms, the pedestrian positioning error will be less than 1 m with a high probability (0.80 when inter-vehicle distance is 40 m and 0.67 when inter-vehicle distance is 70 m). This positioning error also depends on the accuracy of vehicle positions and the accuracy of pedestrian-vehicle distance. Previous works [11] have already shown the possibility of achieving a positioning error of less than 1 m for vehicles in urban areas by integrating different kinds of sensors with satellite signals. The accuracy of pedestrian-vehicle distance depends on the bandwidth of the vehicular signal. In our current evaluation, Wi-Fi (with 20 MHz bandwidth) is used. The performance may get worse when DSRC (with 10 MHz bandwidth) is used. We will further evaluate this in the future.

6 Conclusion

This paper has suggested using moving vehicles as anchors to improve the performance of pedestrian positioning. This is feasible because vehicles will have very accurate position in the era of autonomous driving. However, accurately estimating the distances between vehicles and pedestrians is a challenge. To solve this problem, the proposed method first detects whether LOS path exists for each vehicle and then uses SVR to get a more accurate estimation of distance from CSI instead of RSSI. Vehicles move continuously and periodically transmit signals. This enables frequent measurement of distances at different locations. Together with Kalman filtering, this helps to further improve the positioning performance. Experimental results show that this not only improves the fixing rate but also reduces the average horizontal

This is an open access article published by the IET under the Creative Commons Attribution License
(http://creativecommons.org/licenses/by/3.0/)

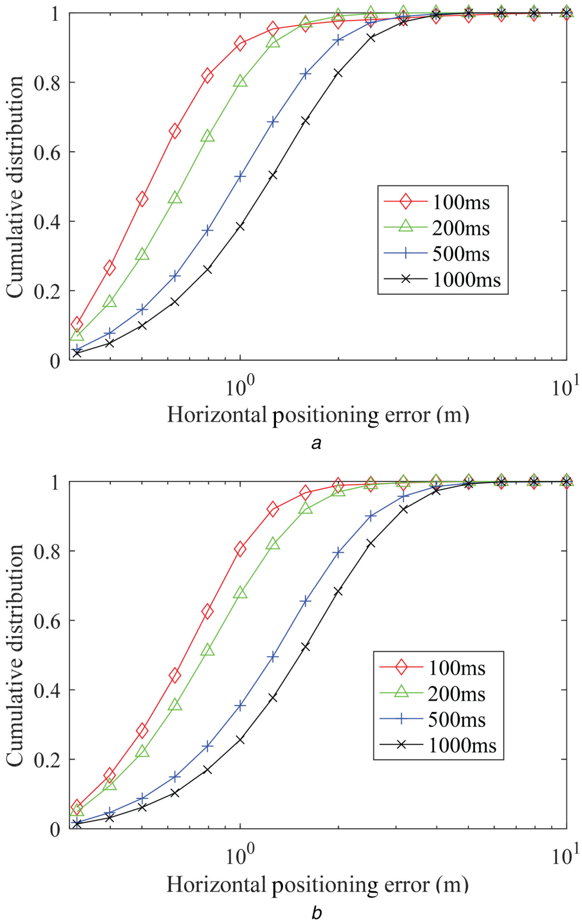

Fig. 9 *Positioning performance under different vehicle transmission periods (The maximal error of vehicle position in the moving direction is set to 1 m.)*
(a) Inter-vehicle distance = 40 m, ***(b)*** Inter-vehicle distance = 70 m

positioning errors to around 80 cm. In addition, the performance of pedestrian positioning improves with the number of vehicles and their transmission frequency.

In the future, we will further leverage deep learning techniques to improve the accuracy of LOS detection and the precision of distance estimation. Current we did not apply Kalman filtering to GPS + CSI, because the distance error property of the GPS receiver is not very stable. We will further study this and also try to do some testbed experiments.

7 Acknowledgment

This work was partly supported by JSPS KAKENHI grant no. 16K00120, and JSPS KAKENHI grant no. 16H02344 Japan.

8 References

[1] 'Annual report of traffic accident statistics (2012 edition)'. Technical Report, Institute for Traffic Accident Research and Data Analysis, 2013
[2] Tang, S., Saito, K., Obana, S.: 'Transmission control for reliable pedestrian-to-vehicle communication by using context of pedestrians'. Proc. IEEE Int. Conf. Vehicular Electronics and Safety (ICVES), 2015, pp. 41–47
[3] Misra, P., Enge, P.: '*Global positioning system: signals, measurements, and performance*' (Ganga-Jamuna, Lincoln MA, 2006, 2nd edn.)
[4] Van, A.J., Fenton, P., Ford, T.: 'Theory and performance of narrow correlator spacing in a GPS receiver', *Navigation, J. Inst. Navig.*, 1992, **39**, (3), pp. 265–283
[5] Betz, J.W.: 'Binary offset carrier modulations for radio navigation', *Navigation, J. Inst. Navig.*, 2001, **48**, (4), pp. 227–246
[6] Hatch, R.: 'The synergism of GPS code and carrier measurements'. Proc. Int. Geodetic Symp. Satellite Doppler Positioning, 1983, pp. 1213–1231
[7] van Nee, R., Siereveld, J., Fenton, P.C., *et al.*: 'The multipath estimating delay lock loop: approaching theoretical accuracy limits'. Proc. IEEE Position Location and Navigation Symp., 1994, pp. 246–251
[8] Rougerie, S., Carrie, G., Vincent, F., *et al.*: 'A new multipath mitigation method for GNSS receivers based on an antenna array', *Int. J. Navig. Obs.*, 2012, **2012**, p. 804732
[9] Suh, Y., Shibasaki, R.: 'Evaluation of satellite-based navigation services in complex urban environments using a three-dimensional GIS', *IEICE Trans. Commun.*, 2007, **E90-B**, (7), pp. 1816–1825
[10] Meguro, J., Murata, T., Takiguchi, J., *et al.*: 'GPS multipath mitigation for urban area using omni directional infrared camera', *IEEE Trans. ITS*, 2009, **10**, (1), pp. 22–30
[11] Gu, Y., Hsu, L.-T., Kamijo, S.: 'Passive sensor integration for vehicle self-localization in urban traffic environment', *Sensors*, 2015, **15**, (12), pp. 30199–30220
[12] Wireless LAN medium access protocol (MAC) and physical layer (PHY) specification. Ammendment 6: Wireless access in vehicular environment, IEEE Std. IEEE Std 802.11p, 2010
[13] 700 MHz band intelligent transport systems, ARIB Std. STD-T109, 2012
[14] Yamashita, R., Tang, S., Obana, S.: 'Improving positioning precision of pedestrians by using both GPS satellites and vehicles'. Proc. ITS World Congress, 2016
[15] Hofmann-Wellenhof, B., Lichtenegger, H., Wasle, E.: '*GNSS – global navigation satellite systems: GPS, GLONASS, Galileo, and more*' (Springer-Verlag, Heidelberg, 2008)
[16] Pratama, A.R., Widyawan Hidayat, R.: 'Smartphone-based pedestrian pedestrian dead reckoning as an indoor positioning system'. Proc. Int. Conf. System Engineering and Technology (ICSET), 2012, pp. 1–6
[17] Yang, Z., Zhou, Z., Liu, Y.: 'From RSSI to CSI: indoor localization via channel response', *ACM Comput. Surv.*, 2013, **46**, (2), pp. 25:1–25:32
[18] Xiao, J., Zhou, Z., Yi, Y., *et al.*: 'A survey on wireless indoor localization from the device perspective', *ACM Comput. Surv.*, 2016, **49**, (2), pp. 25:1–25:31
[19] Wang, X., Gao, L., Mao, S., *et al.*: 'CSI-based fingerprinting for indoor localization: A deep learning approach', *IEEE Trans. Veh. Technol.*, 2017, **66**, (1), pp. 763–776
[20] Sen, S., Lee, J., Kim, K.-H., *et al.*: 'Avoiding multipath to revive inbuilding WiFi localization'. Proc. MobiSys'13, 2013, pp. 249–262
[21] Xie, Y., Li, Z., Li, M.: 'Precise power delay profiling with commodity WiFi'. Proc. MobiCom'15, 2015, pp. 53–64
[22] Vasisht, D., Kumar, S., Katabi, D.: 'Decimeter-level localization with a single WiFi access point'. Proc. NSDI'16, 2016, pp. 165–178
[23] Kotaru, M., Joshi, K., Bharadia, D., *et al.*: 'Spotfi: decimeter level localization using WiFi'. Proc. SIGCOMM'15, 2015, pp. 269–282
[24] Rappaport, T.S.: '*Wireless communications: principles and practice*' (Prentice Hall, Upper Saddle River, 2002, 2nd edn.)
[25] Groves, P.D.: '*Principles of GNSS, inertial, and multi sensor integrated navigation systems*' (Artech House Publishers, Norwood, 2007)
[26] Halperin, D., Hu, W., Sheth, A., *et al.*: 'Tool release: gathering 802.11n traces with channel state information', *SIGCOMM Comput. Commun. Rev.*, 2011, **41**, (1), pp. 53–53

This is an open access article published by the IET under the Creative Commons Attribution License
(http://creativecommons.org/licenses/by/3.0/)